Micellar nanoparticles with tuneable morphologies through interactions between nucleobase-containing synthetic polymers in aqueous solution

Supporting Information

for

Micellar Nanoparticles with Tuneable Morphologies through Interactions between Nucleobase-Containing Synthetic Polymers in Aqueous Solution

Zan Hua,[a] Anaïs Pitto-Barry,[a] Yan Kang,[a] Nigel Kirby,[b] Thomas R. Wilks,[a] and Rachel K. O'Reilly*[a]

[a]Department of Chemistry, University of Warwick, Library Rd., Coventry, CV4 7AL, UK.

[b]Australian Synchrotron, 800 Blackburn Road, Clayton, Victoria 3168, Australia.

Contents

Synthetic Procedures

The synthetic routes to prepare the acrylamide monomers containing the adenine and thymine functionalities are shown in Scheme S1.

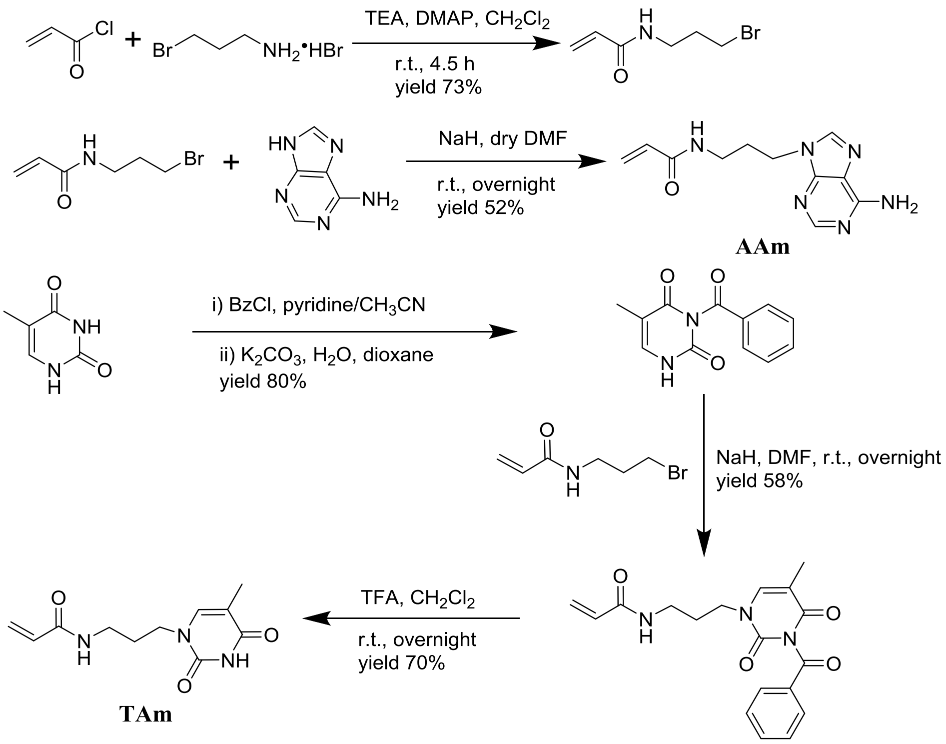

Scheme S1. Syntheses of adenine and thymine acrylamide monomers (AAm and TAm).

Synthesis of *N*-(3-bromopropyl)acrylamide

N-(3-bromopropyl) acrylamide was synthesized using procedures similar to the previous literature.[1] To a solution of 3-bromopropylamine (10.1 g, 45 mmol), triethylamine (TEA) (14 mL, 100 mmol) and 4-(dimethylamino)pyridine (DMAP) (288 mg, 2.3 mmol) in CH_2Cl_2 (150 mL), acryloyl chloride (4.2 mL, 50 mmol) was added dropwise in an ice bath and then left at room temperature for another 4.5 h. The reaction solution was washed with saturated $NaHCO_3$ aqueous solution (100 mL) and water twice sequentially (2 × 100 mL). The organic layer was collected and dried with anhydrous $MgSO_4$ and filtered. Then 2,6-bis(1,1-dimethylethyl)-4-methylphenol (6.3 mg, 1.5 mmol) was added to the filtrate followed by concentrating under vacuum to give a brown oil. The brown oil (6.3 g, 73%) was used for the following reaction immediately without further purification. ^{1}H NMR (400 MHz, $CDCl_3$) δ = 6.27 (d, *J* = 16.8 Hz, 1H, C*H*=CH_2-CO), 6.11 (d, *J* = 10.0 Hz, 1H, C*H*=CH_2-CO), 6.06 (s, 1H, N*H*CO), 5.63 (dd, *J* = 16.8 Hz, 10.0 Hz, 1H, CH_2=C*H*-CO), 3.42-3.50 (m, 4H, CH_2-CH_2-CH_2-Br), 2.08-2.15 (m, 2H, CH_2-CH_2-CH_2-Br) ppm; ^{13}C NMR (400 MHz, $CDCl_3$) δ = 166.0, 130.8, 126.7, 38.2, 32.2, 31.0 ppm.

Synthesis of 3-(adenine-9-yl)propyl acrylamide (AAm)

To a suspension of adenine (3.0 g, 24.2 mmol) in dry DMF (100 mL), NaH (0.85 g, 35.4 mmol) was slowly added. The mixture was stirred for 1 h until no gas was produced. The viscous mixture was immersed into an ice bath and *N*-(3-bromopropyl) acrylamide freshly synthesized (5.4 g, 28.2 mmol) was added dropwise. The yellow viscous mixture was stirred overnight and the resulting suspension was concentrated under vacuum. The solid was washed by CH_2Cl_2 several times and then concentrated. The mixture was further purified by column chromatography using a mixture of CH_2Cl_2 and CH_3OH as eluent and a gradient from 1:0 to 9:1 to give a white solid, AAm (3.18 g, 52%). ^{1}H NMR (400 MHz, DMSO-d_6) δ = 8.19 (t, *J* = 5.2 Hz, CON*H*), 8.15 (s, 1H, purine *H*-2), 8.14 (s, 1H, purine *H*-8), 7.20 (s, 2H, NH_2), 6.21 (dd, *J* = 16.8 Hz, 10.0 Hz, 1H, CH_2=C*H*-CO), 6.08 (dd, *J* = 16.8 Hz, 2.0 Hz, 1H, C*H*=CH_2-CO), 5.59 (dd, *J* = 10.0 Hz, 2.0 Hz, 1H, C*H*=CH_2-CO), 4.15 (t, 2H, *J* =6.8 Hz, CH_2-purine) 3.13 (m, 2H, OC-NH-CH_2), 1.97 (m, 2H, OC-NH-CH_2-CH_2-CH_2-purine) ppm; ^{13}C NMR (400 MHz, DMSO-d_6) δ = 165.6, 153.3, 150.4, 148.3, 141.8, 132.6, 126.1, 119.7, 41.8, 36.8, 30.4 ppm; HR-MS (m/z) found 269.1119, calc. 269.1127 $[M+Na]^+$.

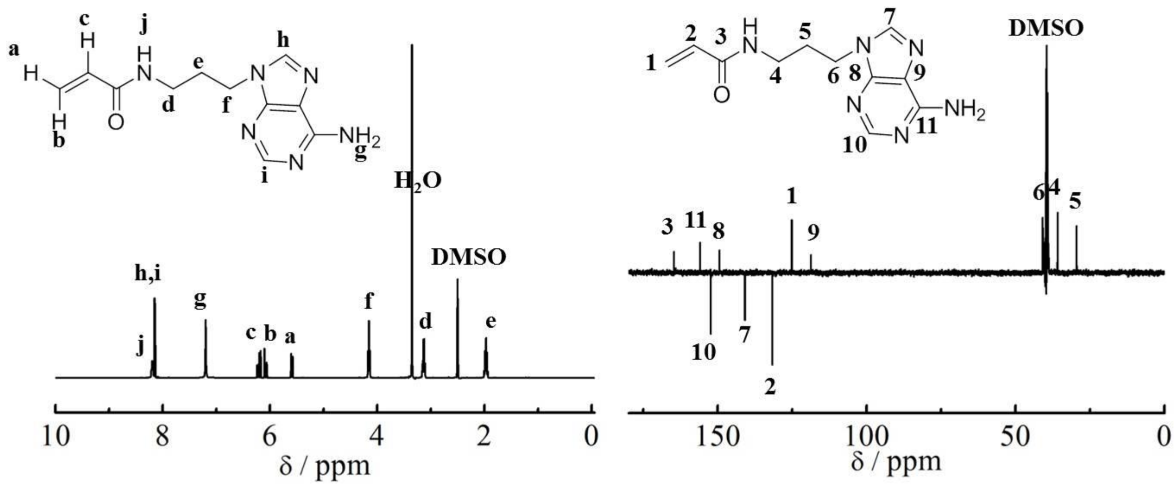

Figure S1. ^{1}H NMR and ^{13}C NMR spectra of 3-(adenine-9-yl)propyl acrylamide (AAm) in DMSO-d_6.

Synthesis of 3-benzoylthymine

Following the procedures in a previous report,[2] benzoyl chloride (11.24 mL, 96.8 mmol) and thymine (3.0 g, 24.2 mmol) were suspended in a mixture of acetonitrile (30 mL) and pyridine (12 mL) under nitrogen. The reaction was stirred under a nitrogen atmosphere at room temperature overnight. The reaction solution was then concentrated under vacuum. The viscous liquid was partitioned between CH_2Cl_2 and water. The aqueous layer was extracted three times with CH_2Cl_2 and the combined organic layers were dried over anhydrous K_2CO_3. The solvent was removed under vacuum. The residue was dissolved in dioxane (30 mL) and K_2CO_3 (4.1 g) in 30 mL of water was added and the reaction mixture was stirred for 2 h. The crude product was concentrated and colourless crystals (4.5 g, 80%) were recrystallized from the solution. ^{1}H NMR (400 MHz, DMSO-d_6) δ = 11.4 (br, 1H, pyrimidine-*H*1), 7.94 (d, *J* = 10.0 Hz, 2H, benzene-*H*1,*H*5), 7.77 (t, *J* = 10.0 Hz, 1H, benzene-*H*3), 7.59 (d, *J* = 10.0 Hz, 2H, benzene-*H*2,*H*4), 7.53 (s, 1H, pyrimidine-*H*6), 1.82 (d, 3H, *J* = 6.8 Hz, CH_3-pyrimidine) ppm; ^{13}C NMR (400 MHz, DMSO-d_6) δ = 170.7, 164.1, 150.5, 139.3, 135.8, 131.9, 130.7, 129.9, 108.4, 12.2 ppm.

Synthesis of 3-(3-benzoylthymin-1-yl)propyl acrylamide

To the solution of 3-benzoylthymine (2.3 g, 10.0 mmol) in dry DMF (50 mL), 60% NaH (0.42 g, 10.5 mmol) was slowly added. The mixture was stirred for 1 h until no gas was produced. The viscous mixture was immersed in an ice bath and *N*-(3-bromopropyl) acrylamide freshly synthesized (2.3 g, 12.0 mmol) was added dropwise. The yellow, viscous mixture was stirred overnight. The resulting solution was concentrated under vacuum. The residue was partitioned with EtOAc and water. The aqueous layer was extracted three times with EtOAc and the combined organic layers were dried over anhydrous $MgSO_4$. The solvent was removed under vacuum. The mixture was further purified by column chromatography using EtOAc as eluent to give a viscous liquid (2.0 g, 58%). ^1H NMR (400 MHz, DMSO-d_6) δ = 8.17 (t, *J* = 5.2 Hz, CON*H*), 7.96 (d, *J* = 6.0 Hz, 2H, benzene-*H*1,*H*5), 7.79 (s, 1H, pyrimidine-*H*6), 7.77 (t, *J* = 6.0 Hz, 1H, benzene-*H*3), 7.59 (d, *J* = 6.0 Hz, 2H, benzene-*H*2, *H*4), 6.20 (dd, *J* = 17.0 Hz, 10.0 Hz, 1H, CH_2=C*H*-CO), 6.10 (dd, *J* = 17.0 Hz, 2.0 Hz, 1H, C*H*=CH_2-CO), 5.58 (dd, *J* = 10.0 Hz, 2.0 Hz, 1H, C*H*=CH_2-CO), 3.73 (t, 2H, *J* = 7.0 Hz, CH_2-pyrimidine), 3.20 (m, 2H, OC-NH-CH_2), 1.84 (d, 3H, *J* = 6.8 Hz, CH_3-pyrimidine), 1.82 (m, 2H, OC-NH-CH_2-CH_2-CH_2-pyrimidine) ppm; ^{13}C NMR (400 MHz, DMSO-d_6) δ = 170.3, 165.2, 163.4, 149.9, 143.0, 135.9, 132.1, 131.7, 130.8, 130.0, 125.6, 109.0, 46.6, 36.3, 28.9, 12.3 ppm.

Synthesis of 3-(thymin-1-yl)propyl acrylamide (TAm)

(3-Benzoylthymin-1-yl)propyl acrylamide (2.0 g, 5.9 mmol) was dissolved in a mixture of TFA/H_2O (3:1) (20 mL) (Scheme 3). The reaction solution was stirred at room temperature overnight. After completion of the reaction, solvent was removed under vacuum. The residue was purified by column chromatography with a gradient of $CHCl_3/CH_3OH$ from 1:0 to 93:7 to give a viscous liquid. Ethanol (20 mL) was then added to give a white solid (1.0 g, 70%). ^1H NMR (500 MHz, DMSO-d_6) δ = 11.23 (s, 1H, pyrimidine-*H*3), 8.12 (t, *J* = 5.2 Hz, CON*H*), 7.51 (s, 1H, pyrimidine-*H*6), 6.18 (dd, *J* = 16.8 Hz, 10.0 Hz, 1H, CH_2=C*H*-CO), 6.07 (dd, *J* = 16.8 Hz, 2.0 Hz, 1H, C*H*=CH_2-CO), 5.58 (dd, *J* = 10.0 Hz, 2.0 Hz, 1H, C*H*=CH_2-CO), 3.63 (t, 2H, *J* = 6.8 Hz, CH_2-pyrimidine), 3.14 (m, 2H, OC-NH-CH_2), 1.74 (d, 3H, *J* = 1.0 Hz, CH_3-pyrimidine), 1.74 (m, 2H, OC-NH-CH_2-CH_2-CH_2-pyrimidine) ppm; ^{13}C NMR (500 MHz, DMSO-d_6) δ = 165.1, 164.8, 151.3, 142.0, 132.2, 125.6, 108.9, 45.9, 36.4, 29.1, 12,4 ppm; HR-MS (m/z) found 260.1004, calc. 260.1011 $[M+Na]^+$.

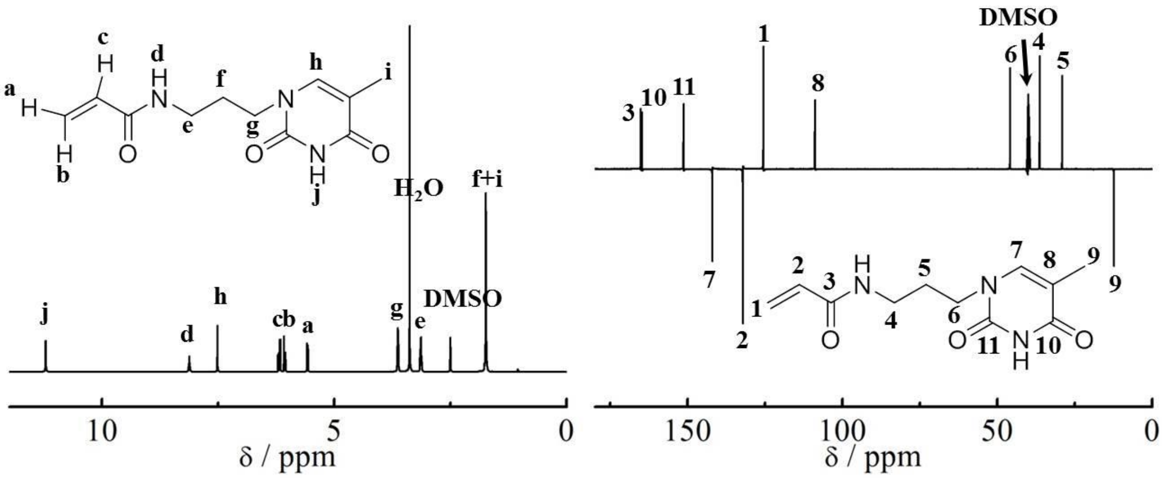

Figure S2. ^1H NMR and ^{13}C NMR spectra of 3-(thymin-1-yl)propyl acrylamide (TAm) in DMSO-d_6.

Synthesis of 2-(((butylthio)carbonothiolyl)thio)propanoic acid (CTA)

The details of the procedures are as follows.[3] A 50% NaOH aqueous solution (8.0 g, containing 4.0 g, 100 mmol of NaOH) was added to a stirred mixture of butanethiol

(10.7 mL, 100 mmol) and water (15 mL). Acetone (5 mL) was then added, and the resulting clear, colorless solution was stirred for 0.5 h then cooled to near-room temperature and treated with carbon disulfide (7.2 mL, 120 mmol) to give a clear orange solution. This was stirred for 0.5 h then cooled in an ice bath to an internal temperature of < 10 °C. 2-Bromopropanoic acid (9.3 mL, 103 mmol) was then added at a slow rate so the temperature did not exceed 30 °C. When the exothermic process had stopped, the ice bath was removed and water (15 mL) was added. The reaction was stirred at ambient temperature for 24 h then diluted with water (25 mL) and cooled in an ice bath while 10 M HCl (15 mL) was added at a rate which kept the temperature < 10 °C. A yellow oil separated and stirring of the mixture was continued at ice temperature until the oil solidified. The solid was collected by suction filtration, pressed and washed with cold water, and dried under reduced pressure to a state of semi-dryness. The lumps were crushed with a spatula; the now-granular solid was resuspended in cold water and stirred for 15 min then refiltered. The residue was washed with cold water and air-dried to afford a powdery yellow solid, which was recrystallized from hexane to give bright yellow crystals (17.2 g, 72%). ^{1}H NMR (400 MHz, $CDCl_3$) δ = 9.82 (br, 1H, COO*H*), 4.87 (q, J = 10.0 Hz, 1H, OC-C*H*-CH_3), 3.37 (t, J = 10.0 Hz, 2H, SC(=S)-CH_2), 1.69 (m, 2H, SC(=S)- CH_2-CH_2), 1.63 (d, J = 10.0 Hz, 3H, OC-CH-CH_3), 1.43 (m, 2H, C$H_2$$CH_3$), 0.93 (t, J = 10.0 Hz, 3H, CH_2CH_3) ppm; ^{13}C NMR (400 MHz, $CDCl_3$) δ = 177.4, 165.2, 47.7, 37.3, 30.1, 22.3, 16.8, 13.8 ppm; HR-MS (m/z) found 237.0082, calc. 237.0078 $[M-H]^-$.

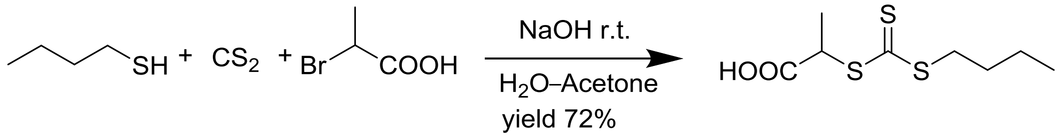

Scheme S2. Synthesis of 2-(((butylthio)carbonothiolyl)thio)propanoic acid (CTA).

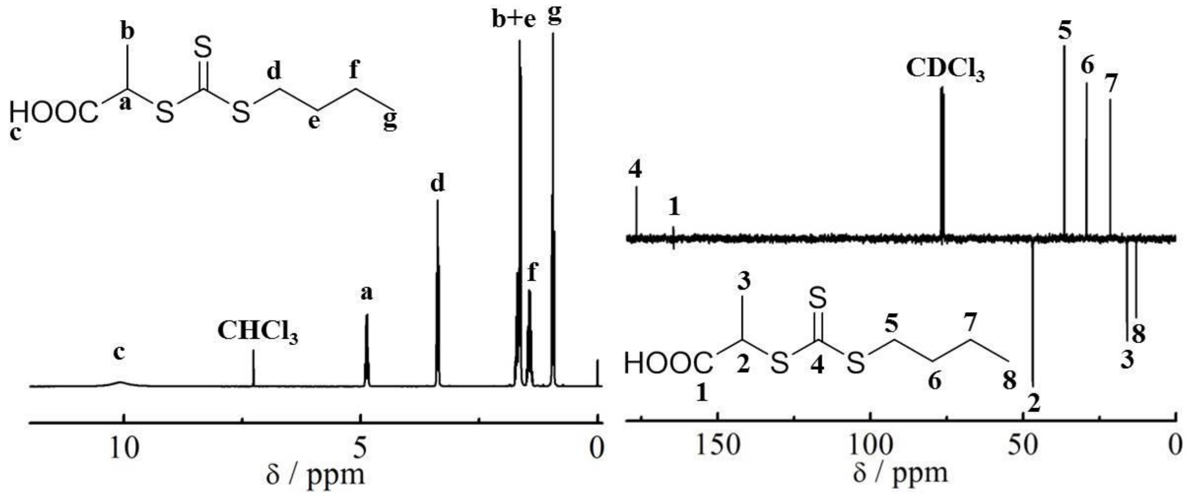

Figure S3. [1]H NMR and [13]C NMR spectra of 2-(((butylthio)carbonothiolyl)thio)propanoic acid (CTA) in $CDCl_3$.

Characterization of the nucleobase-containing diblock copolymers

[1]H NMR spectra of macro-CTA and nucleobase-containing diblock copolymers.

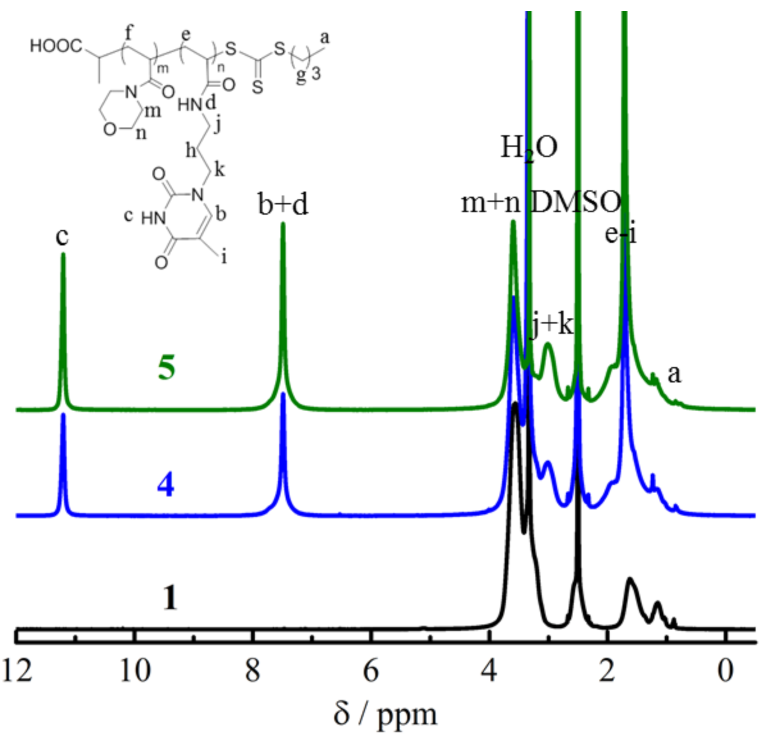

Figure S4. Representative ^{1}H NMR spectra of macro-CTA and nucleobase-containing diblock copolymers in DMSO-d_6.

SEC traces of macro-CTA and nucleobase-containing diblock copolymers

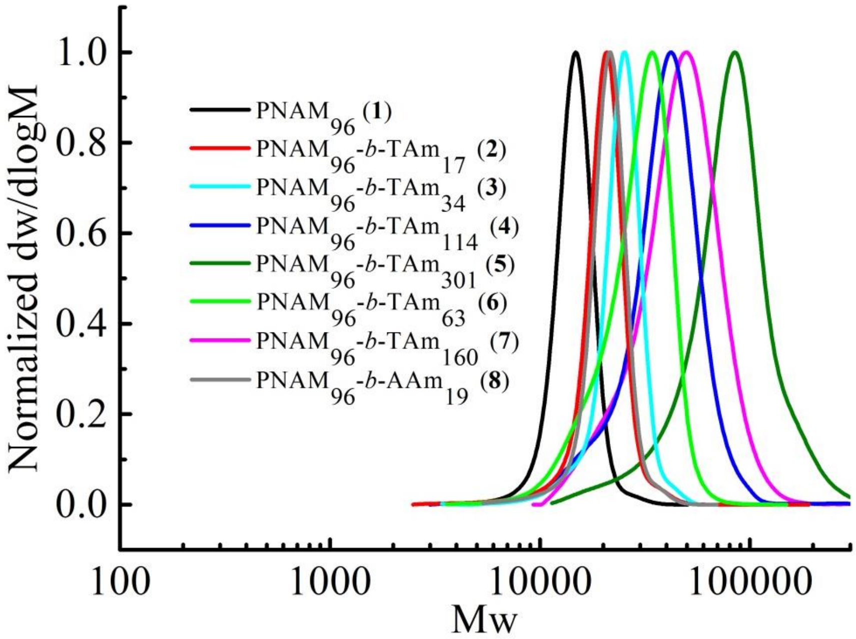

Figure S5. SEC traces (DMF + 5 mM NH_4BF_4 as eluent) of macro-CTA and nucleobase-containing diblock copolymers **1**-**8**.

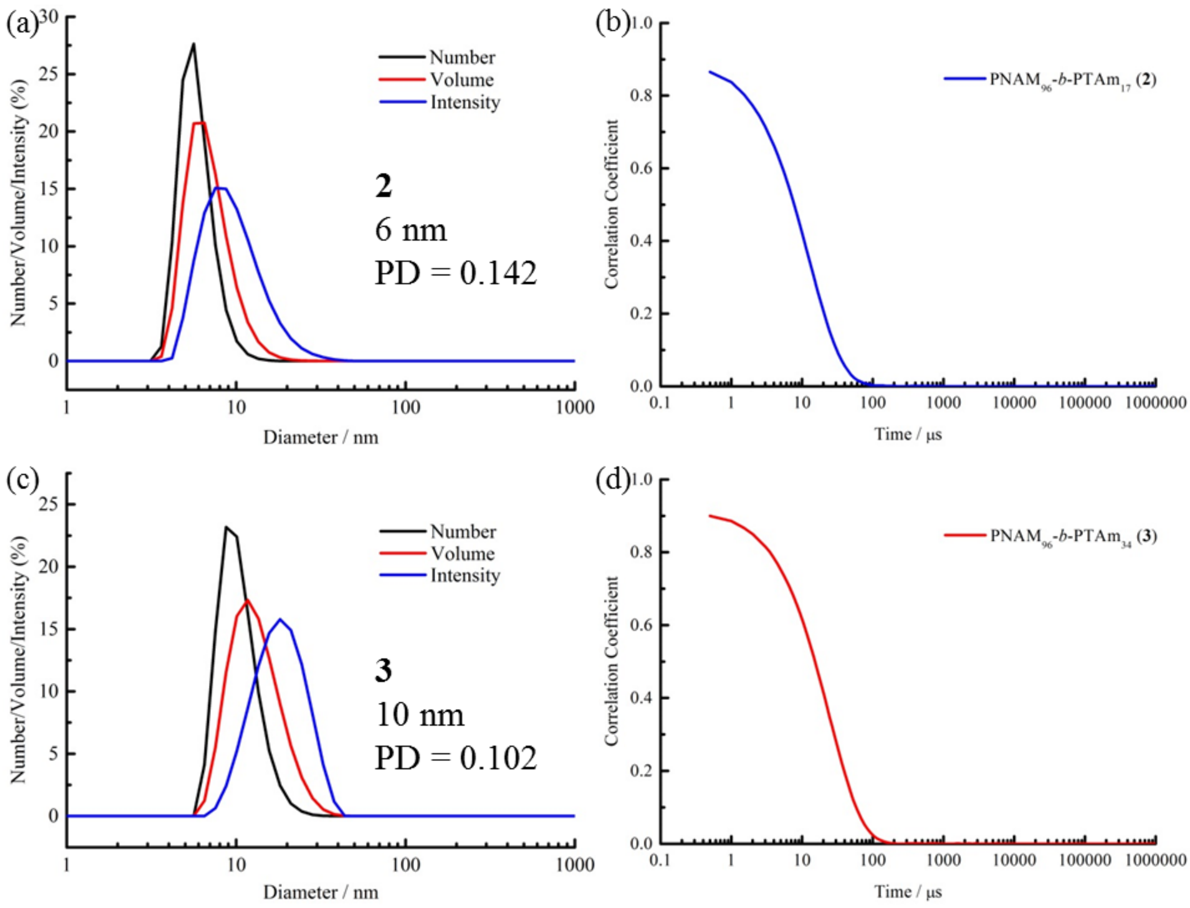

Figure S6. DLS analyses of diblock copolymers in water with short hydrophobic blocks of TAm. (a, b) PNAM$_{96}$-*b*-PTAm$_{17}$ (**2**); (c, d) PNAM$_{96}$-*b*-PTAm$_{34}$ (**3**).

TEM image analyses of PNAM-*b*-PTAm spherical micelles 4-7

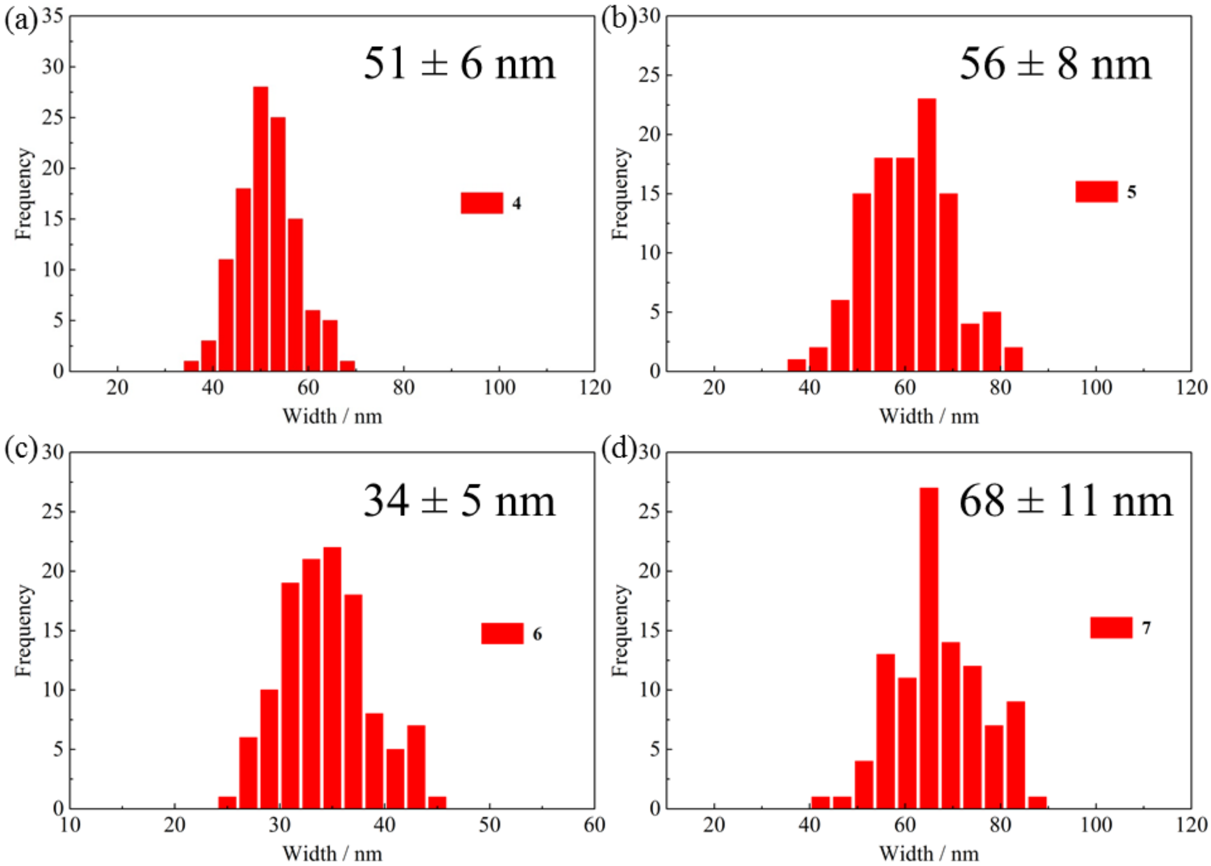

Figure S7. Histograms of the diameters of PNAM-*b*-PTAm spherical micelles of **4-7** as determined by TEM analyses. See Figure 1b, 1d, S13e and S14e for images.

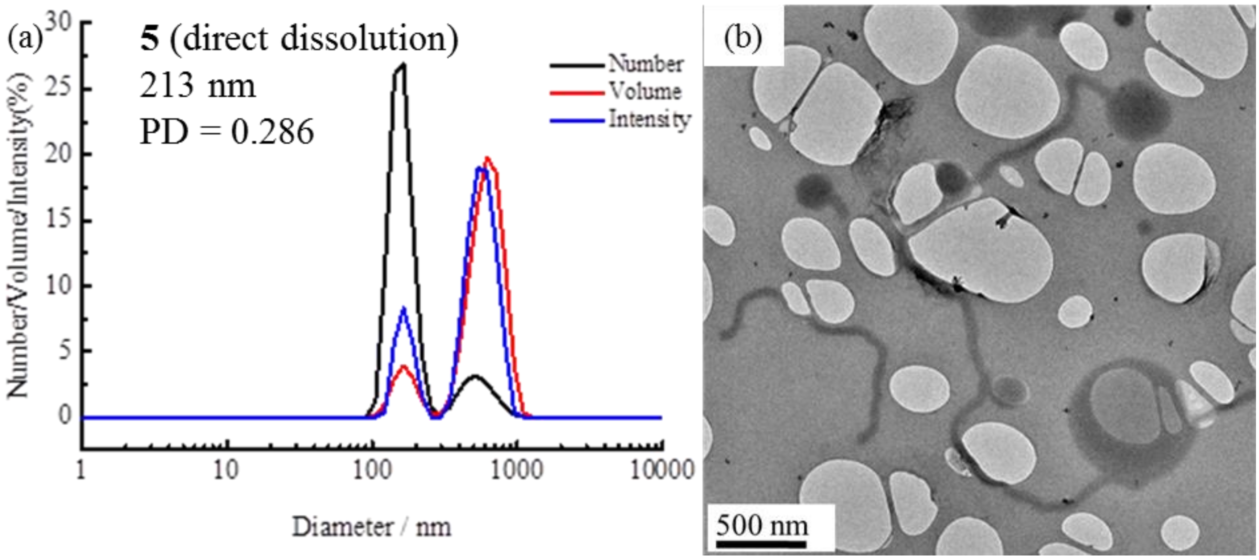

Figure S8. DLS analysis and TEM image of PNAM$_{96}$-*b*-PTAm$_{301}$ (**5**) solution by direct dissolution in water at 70 °C, under overnight stirring.

SLS analyses of spherical micelles of 4 and 5

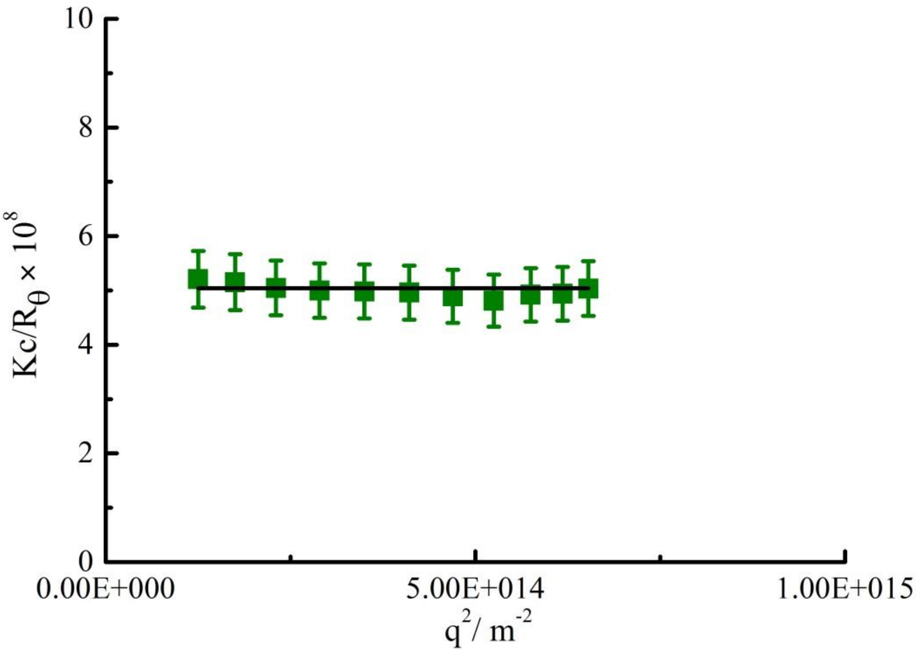

Figure S9. SLS plot of the Rayleigh ratio *vs* q^2 for PNAM$_{96}$-*b*-PTAm$_{114}$ (**4**) micelles in water with 10% error bars. This plot gave M_w = 1.97 × 10^4 kg mol^{-1} and average aggregation number N_{agg} = 390.

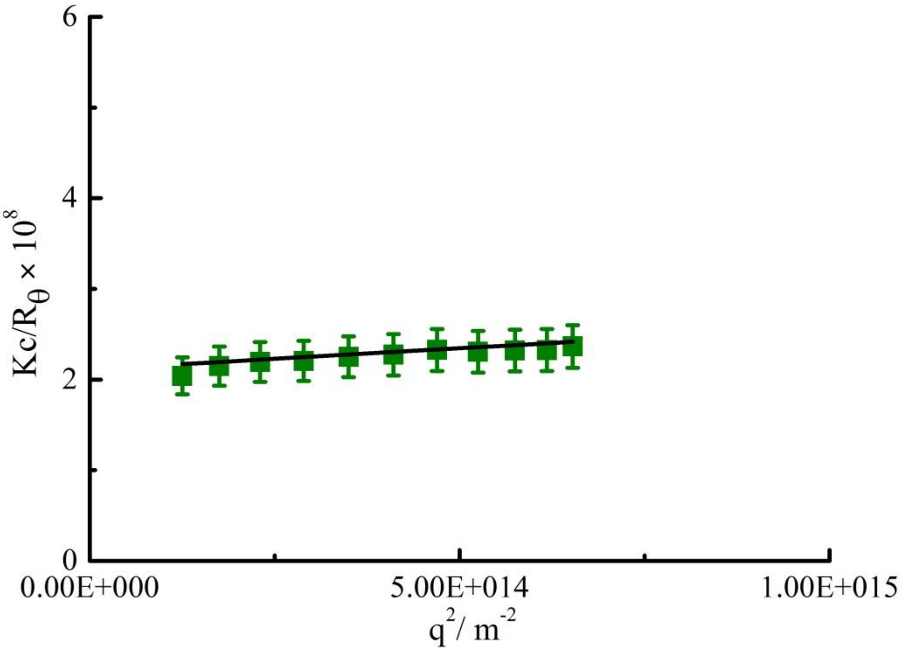

Figure S10. SLS plot of the Rayleigh ratio *vs* q^2 for PNAM$_{96}$-*b*-PTAm$_{301}$ (**5**) micelles in water with 10% error bars. This plot gave M_w = 4.7 × 10^4 kg mol^{-1} and an average aggregation number N_{agg} = 431.

Table S1. Comparison of the diameters and average-aggregation number, N_{agg} for micelles of **4** and **5**.

Sample	D_h[a] (nm)	D_n[b] (nm)	N_{agg}[c]	D_{core}[d] (nm)
4	58	51	390	32
5	57	56	431	47

[a]Measured by DLS. [b]Measured by TEM. [c]Measured by SLS. [d]Core sizes were calculated according to the N_{agg} from SLS.[4]

Characterization of the interactions between micellar solutions of 4, 6 and 7 mixed with different molar ratios of 8

DLS and TEM analyses of the interactions between micellar solutions of 4, 6 and 7 mixed with different molar ratios of 8

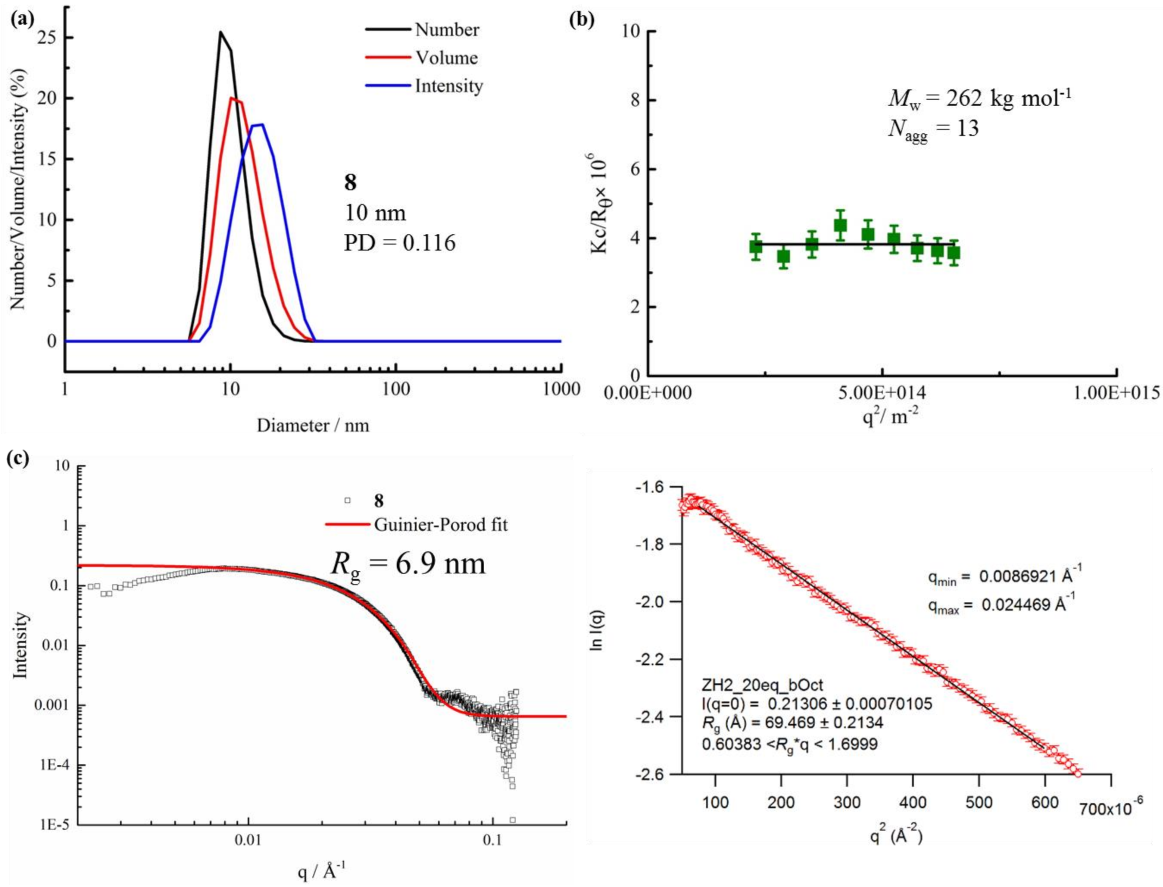

Figure S11. The characterization of the copolymer **8** in H_2O by DLS, SLS and SAXS.

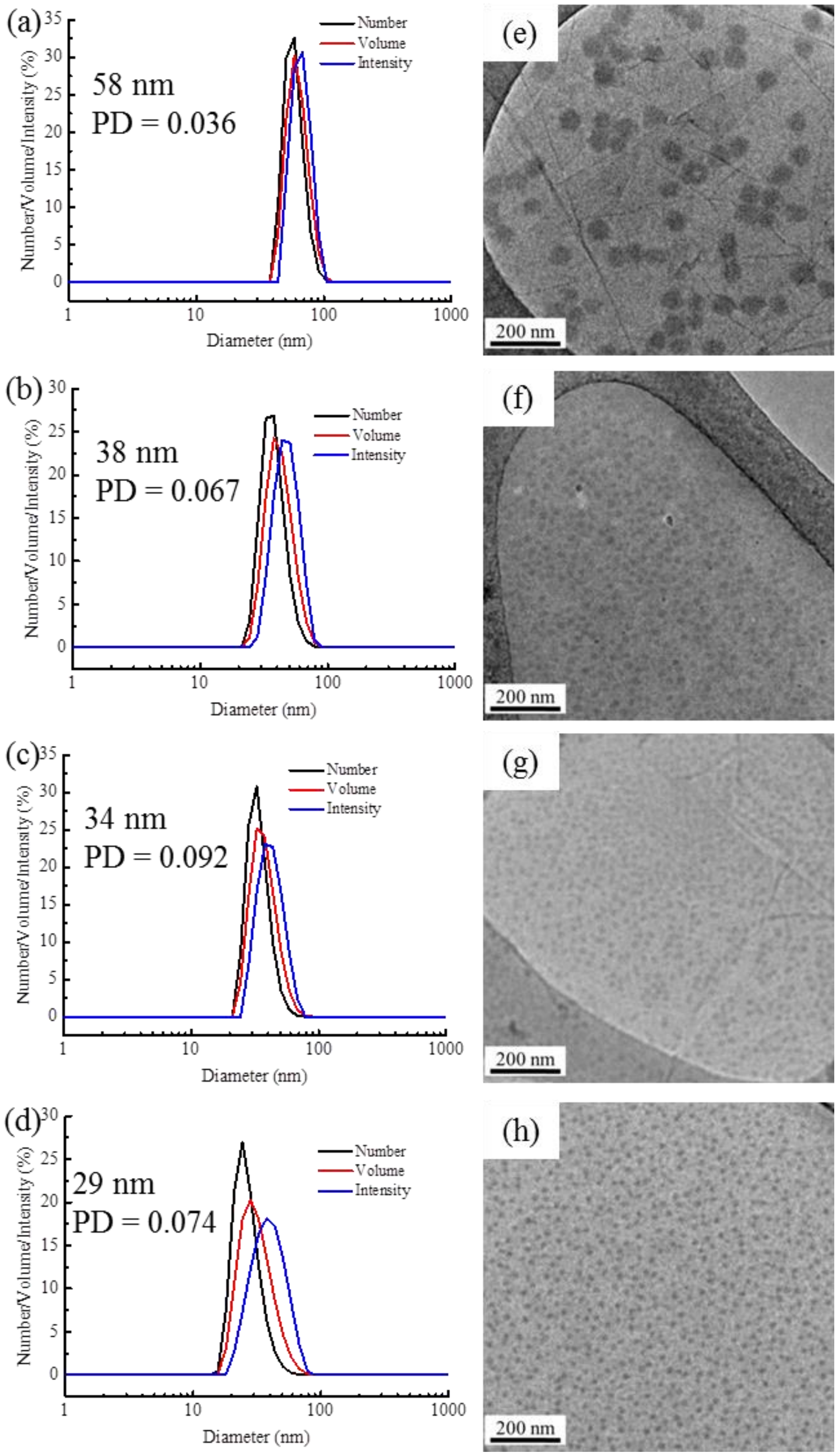

Figure S12. DLS analyses and TEM images of PNAM$_{96}$-*b*-PTAm$_{114}$ (**4**) micelle solution mixed with different molar ratios of PNAM$_{96}$-*b*-PAAm$_{19}$ (**8**). (a, e) 0 molar eq., (b, f) 1 molar eq., (c, g) 3 molar eq., (d, h) 5 molar eq. of PNAM$_{96}$-*b*-PAAm$_{19}$ (**8**).

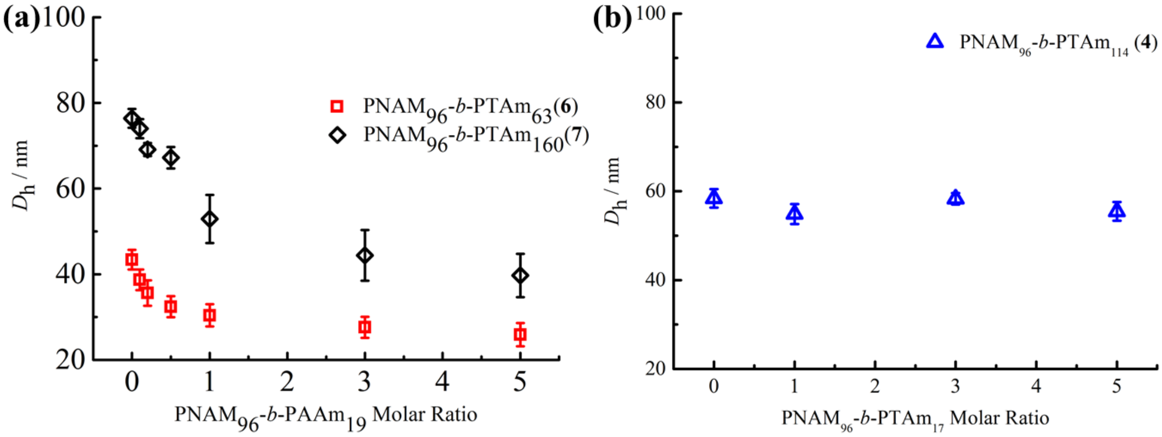

Figure S13. (a) DLS data of PNAM$_{96}$-*b*-PTAm$_{63}$ (**6**) or PNAM$_{96}$-*b*-PTAm$_{160}$ (**7**) micelle solutions mixed with different molar ratios of PNAM$_{96}$-*b*-PAAm$_{19}$ (**8**); (b) DLS data of PNAM$_{96}$-*b*-PTAm$_{114}$ (**4**) micelle solutions mixed with different molar ratios of the non-complementary copolymer PNAM$_{96}$-*b*-PTAm$_{17}$ (**2**).

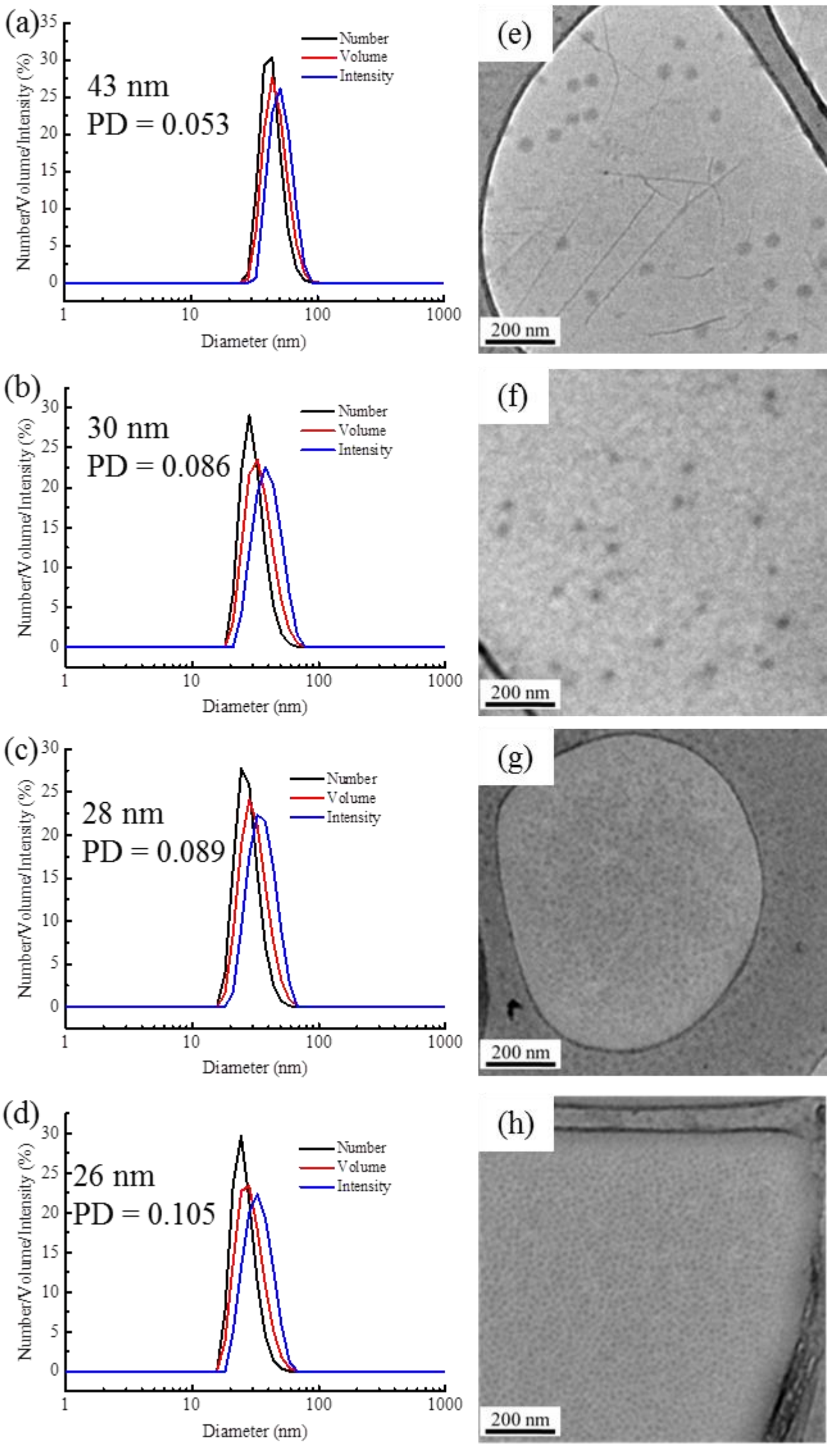

Figure S14. DLS analyses and TEM images of PNAM$_{96}$-*b*-PTAm$_{63}$ (**6**) micelle solution mixed with different molar ratios of PNAM$_{96}$-*b*-PAAm$_{19}$ (**8**). (a, e) 0 molar eq., (b, f) 1 molar eq., (c, g) 3 molar eq., (d, h) 5 molar eq. of PNAM$_{96}$-*b*-PAAm$_{19}$ (**8**).

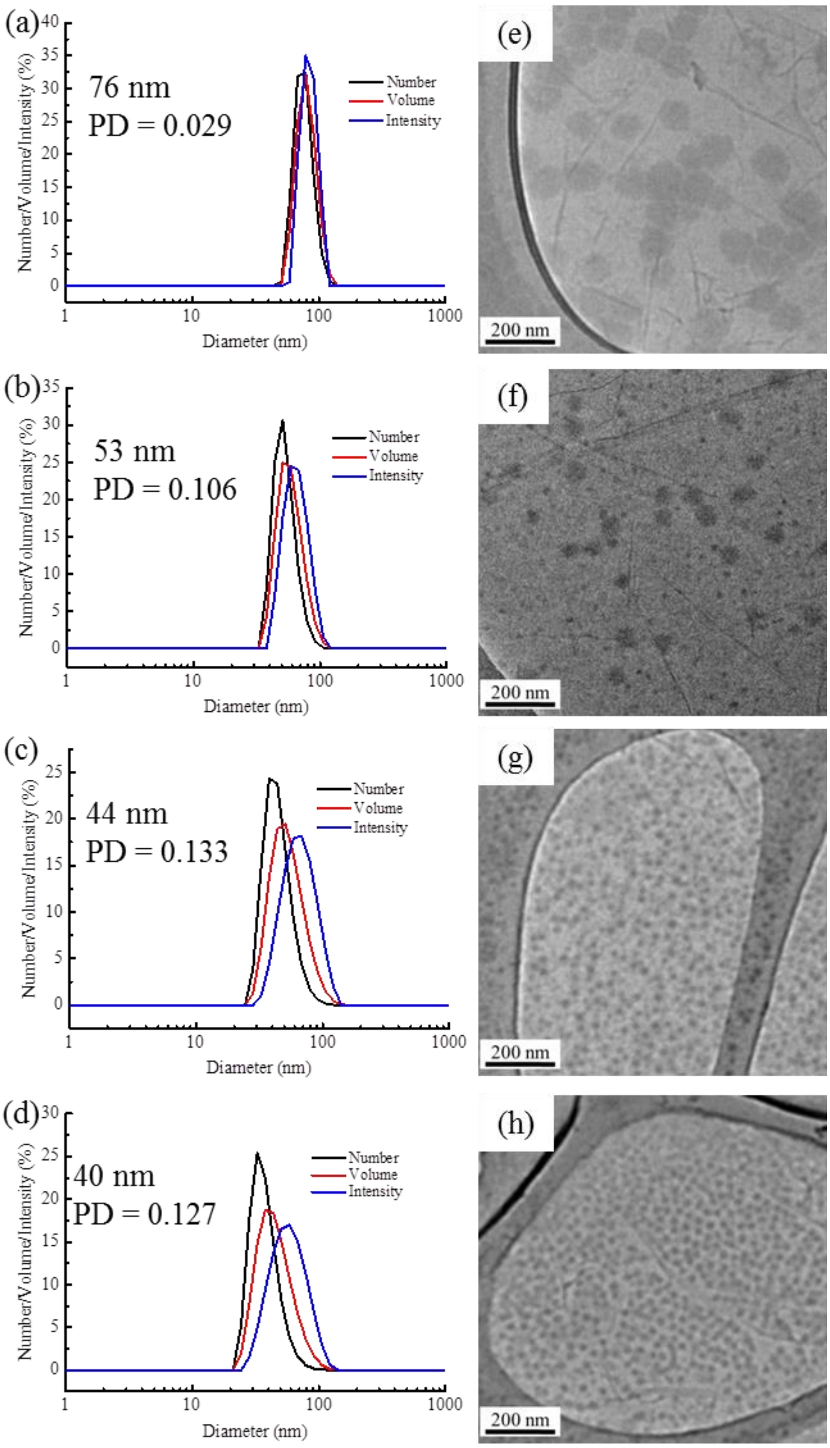

Figure S15. DLS analyses and TEM images of PNAM$_{96}$-*b*-PTAm$_{160}$ (**7**) micelle solutions mixed with different molar ratios of PNAM$_{96}$-*b*-PAAm$_{19}$ (**8**). (a, e) 0 molar eq., (b, f) 1 molar eq., (c, g) 3 molar eq., (d, h) 5 molar eq. of PNAM$_{96}$-*b*-PAAm$_{19}$ (**8**).

[1]H NMR spectra of the interactions between micellar solutions of 4 mixed with different molar ratios of 8

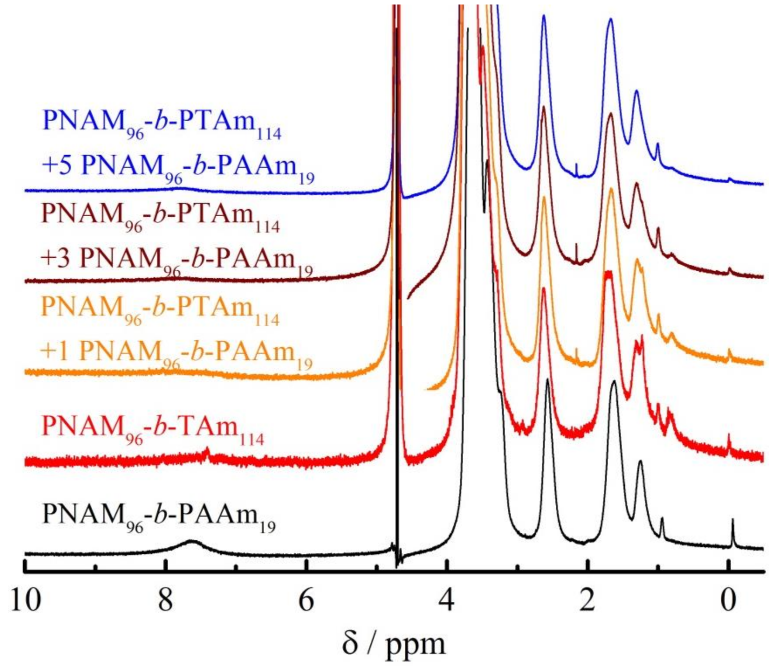

Figure S16. ^{1}H NMR spectra of PNAM$_{96}$-*b*-PAAm$_{19}$ (**8**), PNAM$_{96}$-*b*-PTAm$_{114}$ (**4**) micelle solution and their mixtures at different molar ratios in D_2O.

UV-vis experiments of the interactions between micellar solutions of 4 mixed with different molar ratios of 8

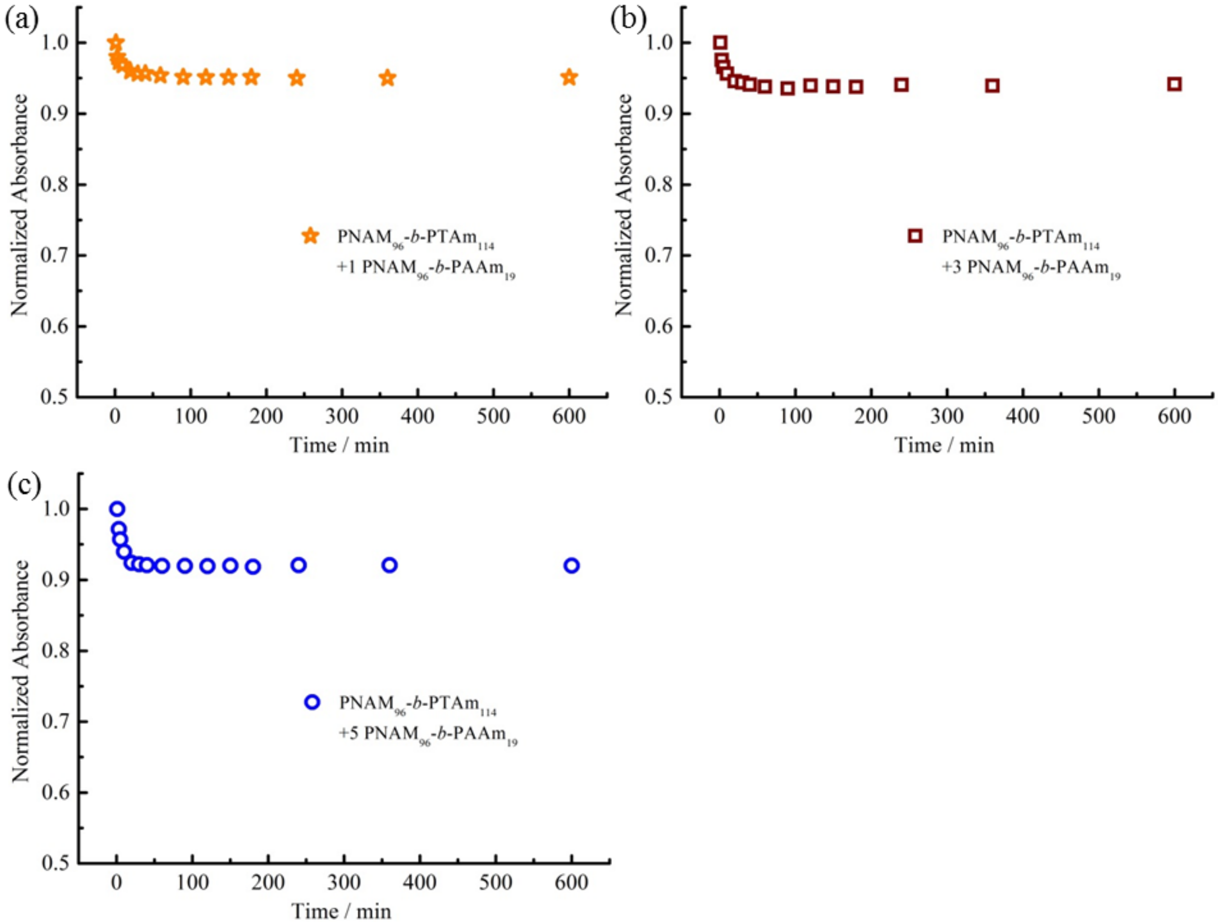

Figure S17. The peak absorbance of UV-vis measurements of the mixture of PNAM$_{96}$-*b*-PTAm$_{114}$ (**4**) micelle solutions mixed with different molar ratios of PNAM$_{96}$-*b*-PAAm$_{19}$ (**8**) at different times. (a) 1 molar eq., (b) 3 molar eq., (c) 5 molar eq. of PNAM$_{96}$-*b*-PAAm$_{19}$ (**8**).

SAXS experiments of the interactions between micellar solutions of 4 mixed with different molar ratios of 8

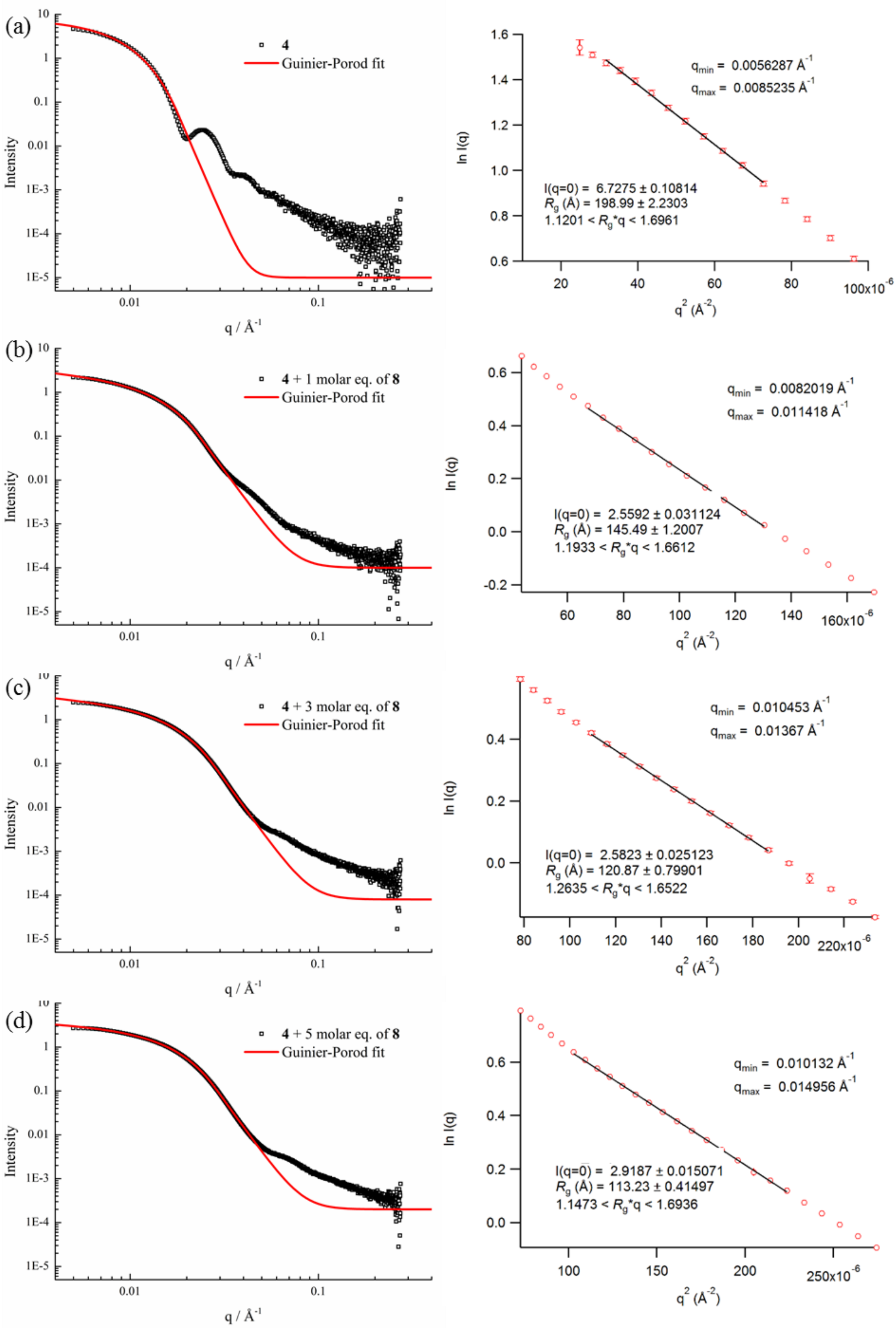

Figure S18. SAXS raw profiles, Guinier-Porod fits (left) and Guinier fits (right) for micellar solutions of **4** mixed with different molar ratios of **8**. (a) 0 molar eq., (b) 1 molar eq., (c) 3 molar eq., (d) 5 molar eq of **8**.

Table S2. Different parameters of the fitted SAXS profiles given in Figure 4a using the Guinier fit and the Guinier-Porod fit.

Sample	R_g (nm)	s[a]	R_g/R_h[b]	R_{core} (nm)[c]
4	19.9	0	0.74	15.4
4 with 1 molar eq. of **8**	14.5	0.38	0.77	7.0
4 with 3 molar eq. of **8**	12.1	0.37	0.71	4.2
4 with 5 molar eq. of **8**	11.3	0.24	0.78	4.2

[a]s = 0: spheres; s = 1: cylinders; s = 2: platelets.[b]R_g/R_h values related to morphology. R_g/R_h = 0.775: spherical micelles; R_g/R_h = 1: vesicles; R_g/R_h > 1: cylinders; R_g and R_h were determined by SAXS and DLS, respectively. [c]R_{core} values were calculated from the N_{agg} from SAXS.

Characterization of the interactions between micellar solutions of 5 mixed with different molar ratios of 8

DLS and TEM analyses of the interactions between micellar solutions of 5 mixed with different molar ratios of 8

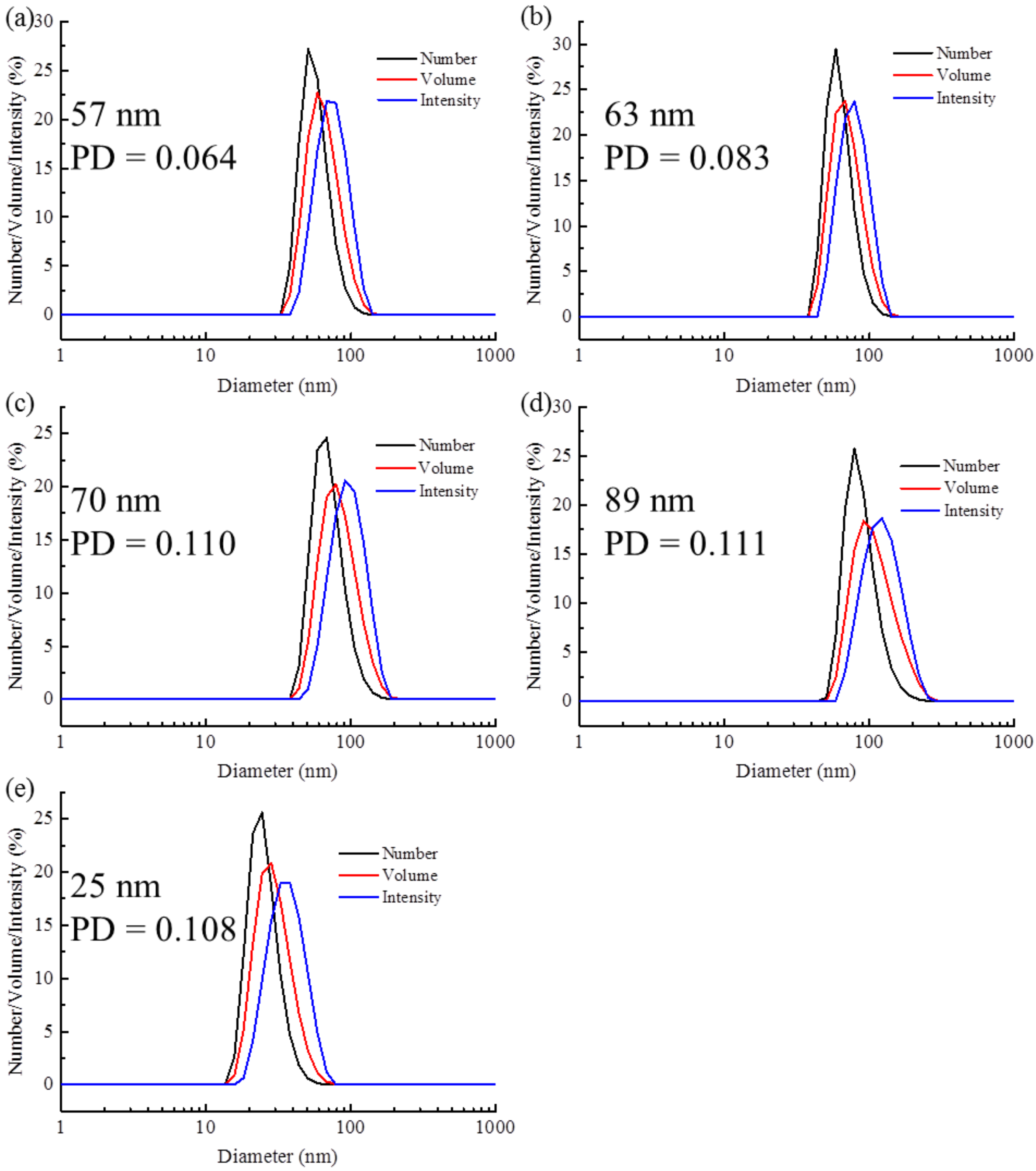

Figure S19. DLS analyses of $PNAM_{96}$-*b*-$PTAm_{301}$ (**5**) micelle solutions mixed with different molar ratios of $PNAM_{96}$-*b*-$PAAm_{19}$ (**8**). (a) 0 molar eq., (b) 1 molar eq., (c) 3 molar eq., (d) 5 eq., (e) 20 molar eq. of $PNAM_{96}$-*b*-$PAAm_{19}$ (**8**).

^{1}H NMR spectra of the interactions between micellar solutions of 5 mixed with different molar ratios of 8

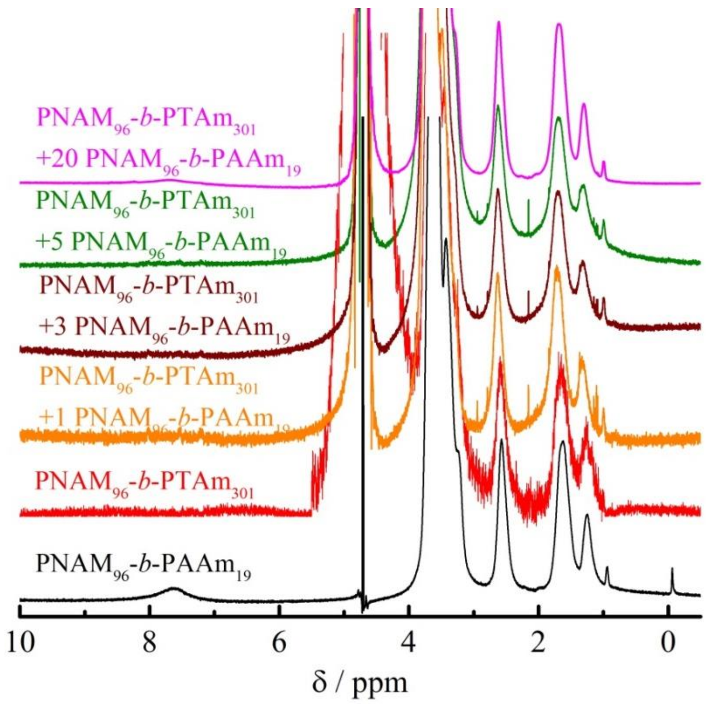

Figure S20. ^{1}H NMR spectra of $PNAM_{96}$-*b*-$PAAm_{19}$ (**8**), $PNAM_{96}$-*b*-$PTAm_{301}$ (**5**) micelle solution and their mixtures at different molar ratios in D_2O.

UV-vis experiments of the interactions between micellar solutions of 5 mixed with different molar ratios of 8

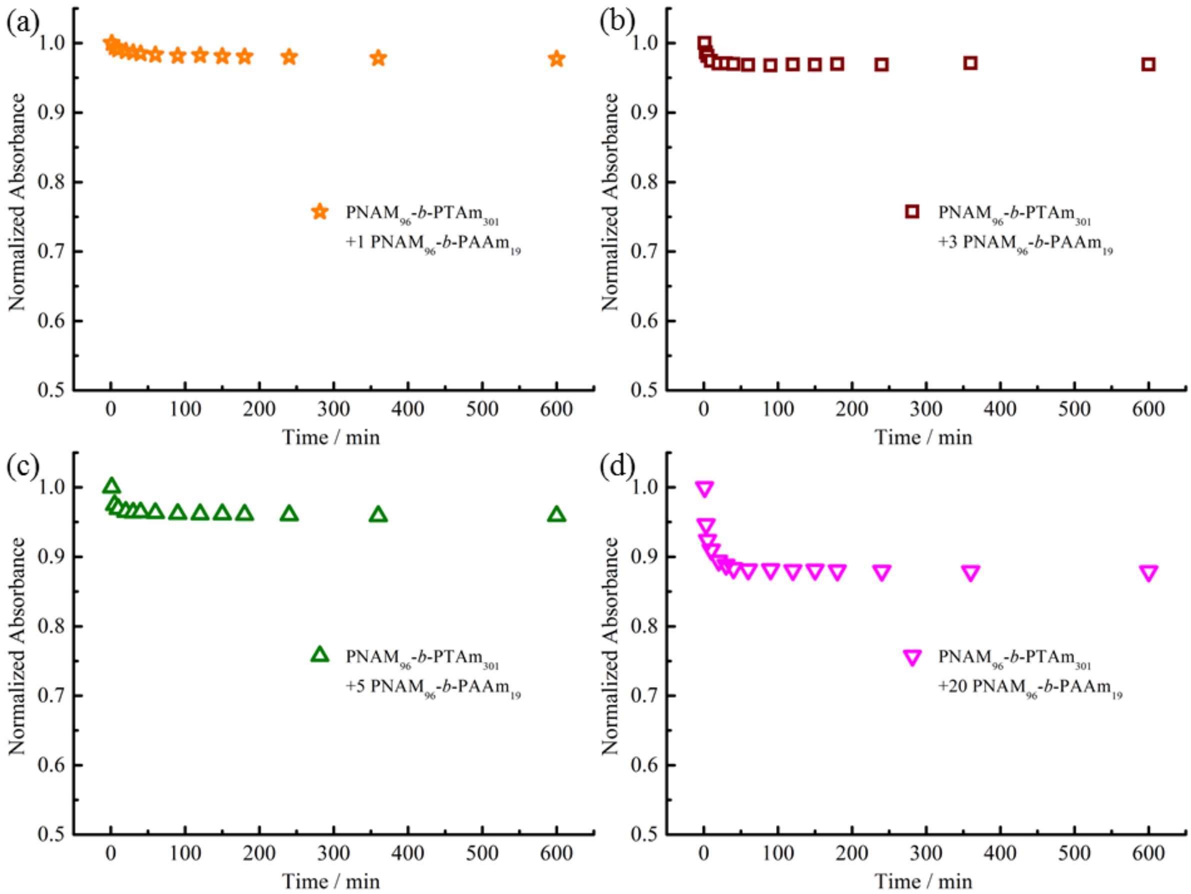

Figure S21. The peak absorbance of UV-vis measurements of the mixture of PNAM$_{96}$-*b*-PTAm$_{301}$ (**5**) micelle solutions with different ratios of PNAM$_{96}$-*b*-PAAm$_{19}$ (**8**) at different time points. (a) 1 molar eq., (b) 3 molar eq., (c) 5 molar eq., (d) 20 molar eq. PNAM$_{96}$-*b*-PAAm$_{19}$ (**8**).

SAXS experiments of the interactions between micellar solutions of 5 mixed with different molar ratios of 8

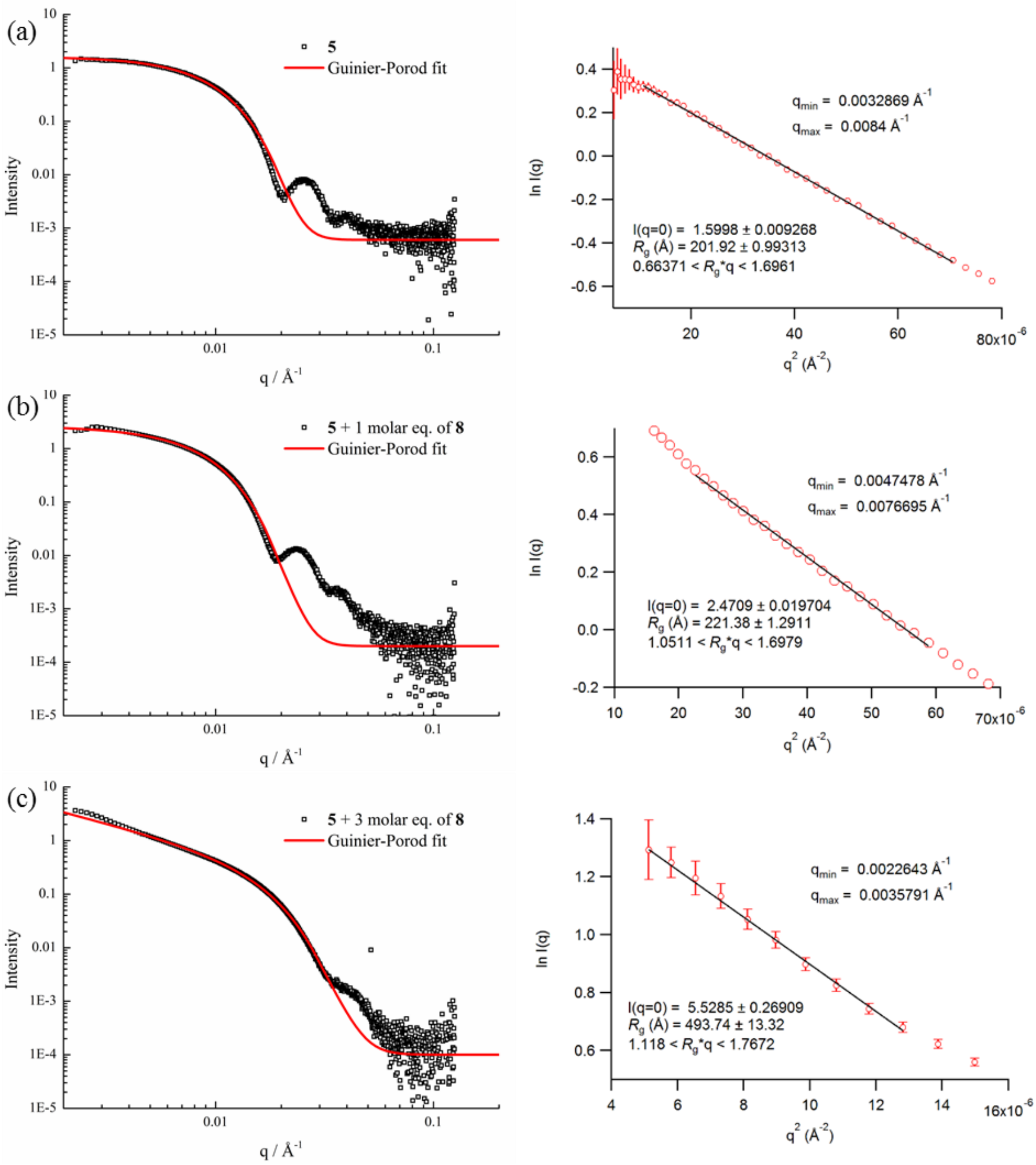

For cylindrical objects, two Guinier regions are determined:

- At low q values, with the slope of the ln I(q) *vs* q^2 equivalent to $-R_g^2/3$, and $R_g^2 = L^2/12 + R^2/2$
- At medium q values, with the slope of ln (q*I(q)) *vs* q^2 equivalent to $-R_g^2/2$, and $R_g^2 = R^2/2$

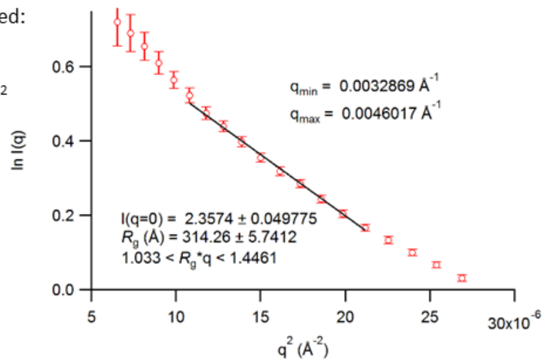

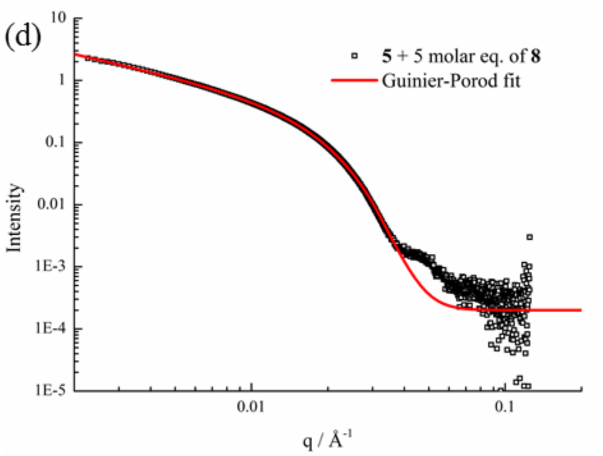

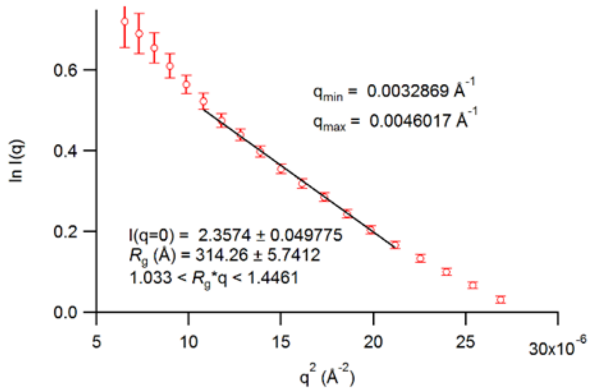

For cylindrical objects, two Guinier regions are determined:

- At low q values, with the slope of the ln I(q) *vs* q^2 equivalent to $-R_g^2/3$, and $R_g^2 = L^2/12 + R^2/2$
- At medium q values, with the slope of ln (q*I(q)) *vs* q^2 equivalent to $-R_g^2/2$, and $R_g^2 = R^2/2$

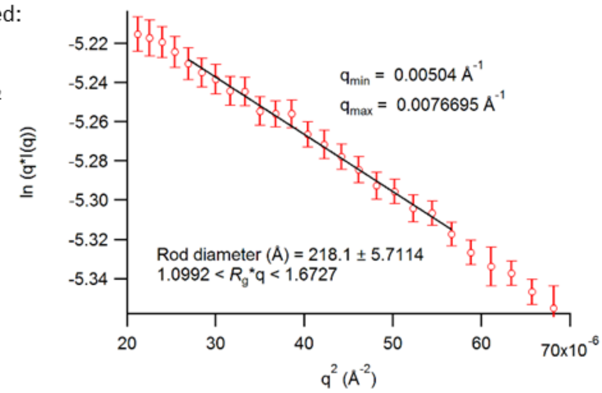

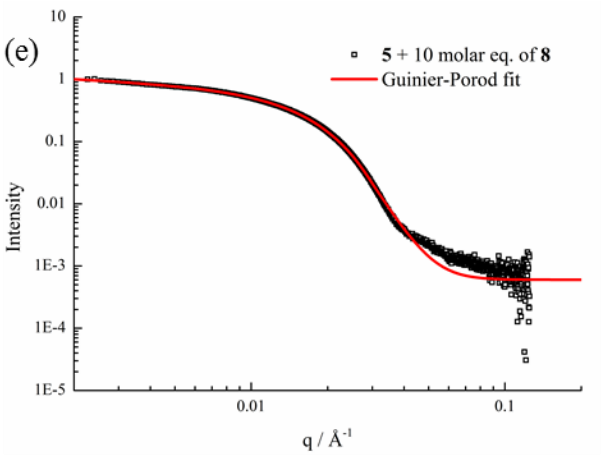

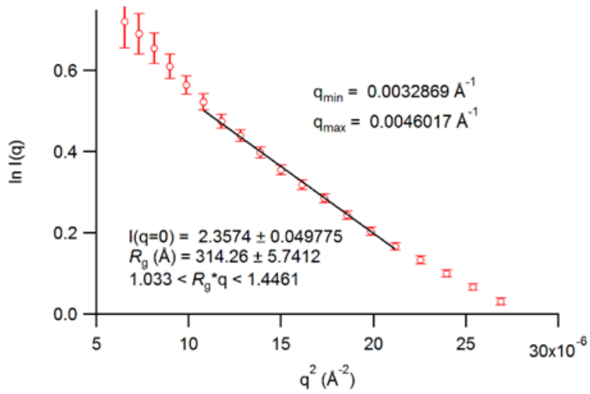

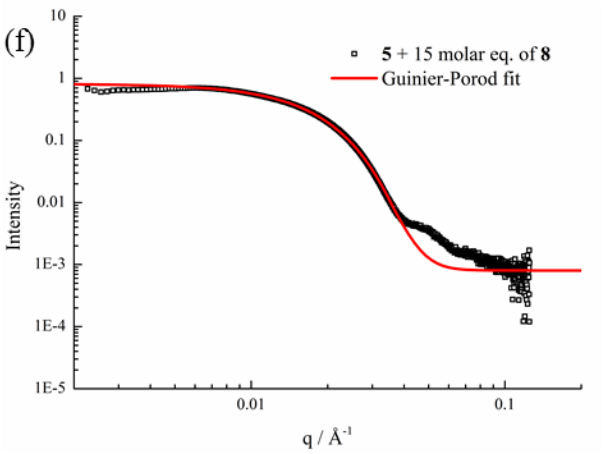

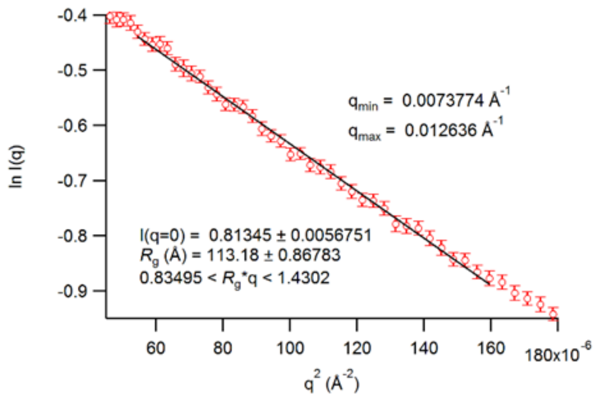

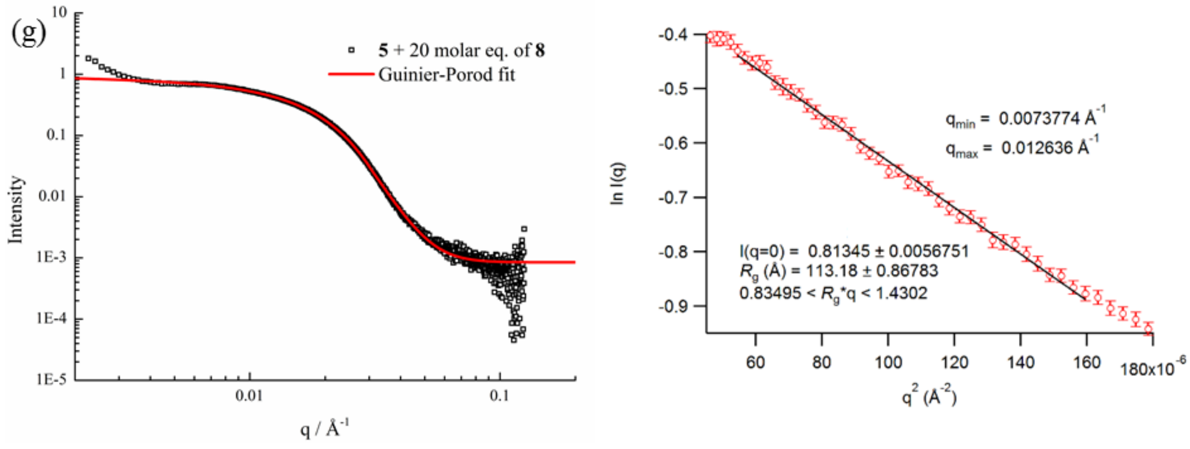

Figure S22. SAXS raw profiles, Guinier-Porod fits (left) and Guinier fits (right) for micellar solutions of **5** mixed with different molar ratios of **8**. (a) 0 molar eq., (b) 1 molar eq., (c) 3 molar eq., (d) 5 molar eq., (e) 10 molar eq., (f) 15 molar eq., (g) 20 molar eq. of **8**.

Table S3. Different parameters of the fitted SAXS profiles given in Figure S21 using Guinier fit and Guinier-Porod fit.

Sample	R_g (nm)	s[a]	R_g/R_h[b]
5	20.2	0	0.71
5 with 1 molar eq. of **8**	22.1	0.07	0.70
5 with 3 molar eq. of **8**	L = 166.7 W = 31.4[c]	1.05	1.38
5 with 5 molar eq. of **8**	L = 105.5 W = 21.8[c]	0.91	1.64
5 with 10 molar eq. of **8**	13.0	0.21	0.75
5 with 15 molar eq. of **8**	10.1	0	0.67
5 with 20 molar eq. of **8**	11.3	0.1	0.81

[a]s = 0: spheres; s = 1: cylinders; s = 2: platelets.[b]R_g/R_h values related to morphology. R_g/R_h = 0.775: spherical micelles; R_g/R_h = 1: vesicles; R_g/R_h > 1: cylinders; R_g and R_h were determined by SAXS and DLS for spherical micelles and R_g was determined by SLS for cylinders. [c]Length and width are fitted from SAXS data using the Guinier fit.

Calculation of the molar ratios of complementary copolymers

The degree of polymerization (DP) of PNAM$_{96}$-*b*-PAAm$_{19}$ (**8**), PNAM$_{96}$-*b*-PTAm$_{114}$ (**4**) and PNAM$_{96}$-*b*-PTAm$_{301}$ (**5**) were obtained from ^{1}H NMR spectroscopic analysis. The number-average molecular weight M_n of the polymers can be calculated from the DP. The self-assemblies of PNAM$_{96}$-*b*-PTAm$_{114}$ (**4**) or PNAM$_{96}$-*b*-PTAm$_{301}$ (**5**) were prepared and the mass concentration is known as *c*. So the molar concentration can be calculated. Then, the mass *m* of PNAM$_{96}$-*b*-PAAm$_{19}$ (**8**) with the relative molar ratios *n* were calculated according to PNAM$_{96}$-*b*-PTAm$_{114}$ (**4**) and PNAM$_{96}$-*b*-PTAm$_{301}$ (**5**) mass concentration and the volume *v* using Eq. 1.

$$m = \frac{ncvM_{n,\mathbf{8}}}{M_{n,\mathbf{4}}} \tag{1}$$

Therefore, the molar ratios $R_{\mathrm{A:T}}$ of complementary nucleobases A and T can also be calculated using the DPs of the AAm and TAm blocks as follows:

$$R_{\mathrm{A:T}} = n\frac{DP(A)_{\mathbf{8}}}{DP(T)_{\mathbf{4}}} \tag{2}$$

Where $DP(A)_{\mathbf{8}}$ is the degree of polymerization of the AAm block in polymer **8**, and $DP(T)_{\mathbf{4}}$ is the degree of polymerization of the TAm block in polymer **4**. Using molar ratios of complementary copolymers or nucleobases, the micellar size change both shows the same trend (Figure S23).

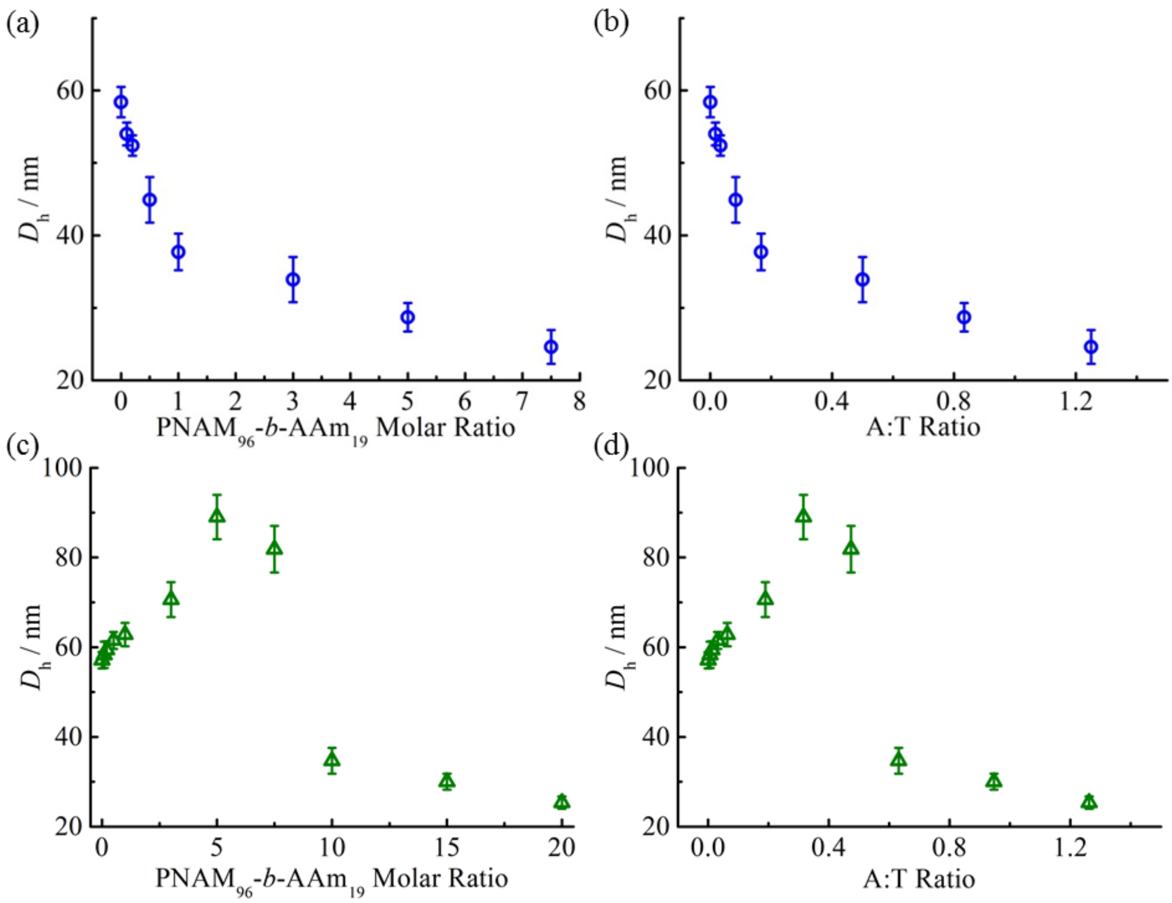

Figure S23. DLS hydrodynamic diameters (D_h) of micellar solutions of **4** and **5** with increasing quantity of **8**. (a,b) D_h of micellar solutions of **4** with increasing quantity of **8** using copolymer molar ratio and A:T ratio, respectively; (c,d) D_h of micellar solutions of **5** with increasing quantity of **8** using copolymer molar ratio and A:T ratio, respectively**.**

References

(1) R. E. Kohman, C. Cha, S. C. Zimmerman and H. Kong, *Soft Matter*, 2010, **6**, 2150-2152.

(2) S. Racine, F. De Nanteuil, E. Serrano and J. Waser, *Angew. Chem., Int. Ed.*, 2014, **53**, 8484-8487.

(3) C. J. Ferguson, R. J. Hughes, D. Nguyen, B. T. T. Pham, R. G. Gilbert, A. K. Serelis, C. H. Such and B. S. Hawkett, *Macromolecules*, 2005, **38**, 2191-2204.

(4) L. D. Blackman, D. B. Wright, M. P. Robin, M. I. Gibson and R. K. O'Reilly, *ACS Macro Lett.*, 2015, **4**, 1210-1214.